AD-A062 698 NORTHWESTERN UNIV EVANSTON IL DEPT OF MATERIALS SCIENCE F/G 11/6
RELATION OF STRUCTURE TO FATIGUE PROPERTIES IN ALUMINUM-BASE AL--ETC(U)
NOV 78 M E FINE AFOSR-76-2892

UNCLASSIFIED AFOSR-TR-78-1518 NL

OF
AD
A062 698

END
DATE
FILMED
3-79
DDC

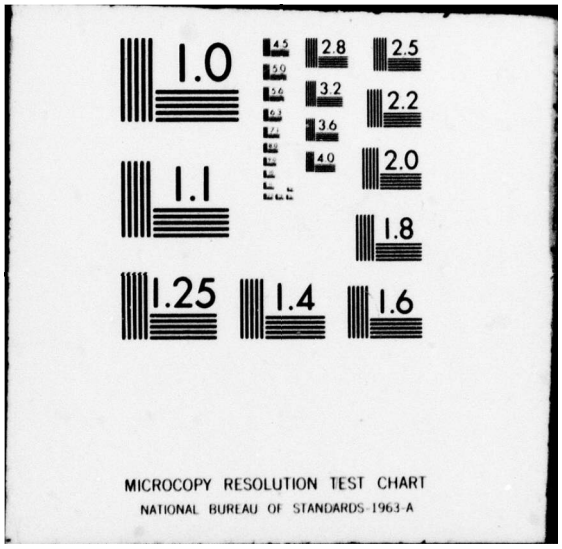
1.0
1.1
1.25
1.4
1.6
1.8
2.0
2.2
2.5
2.8
3.2
3.6
4.0
4.5
5.0
5.6
6.3
7.1
MICROCOPY RESOLUTION TEST CHART
NATIONAL BUREAU OF STANDARDS-1963-A

AFOSR-TR- 78-1518

LEVEL II

FINAL REPORT

on

RELATION OF STRUCTURE TO FATIGUE PROPERTIES IN ALUMINUM-BASE ALLOYS

covering period

01 October 1975 to 30 September 1978

by

Morris E. Fine

30 November 1978

This research was supported by Air Force Office of Scientific Research, Air Force Systems Command USAF under Grant No. AFOSR-76-2892

DEPARTMENT OF MATERIALS SCIENCE AND ENGINEERING
THE TECHNOLOGICAL INSTITUTE
NORTHWESTERN UNIVERSITY
EVANSTON, ILLINOIS 60201

Qualified requestors may obtain additional copies from the Defense Documentation Center; all others should apply to the Clearinghouse for Federal Scientific and Technical Information.

AIR FORCE OFFICE OF SCIENTIFIC RESEARCH (AFSC)
NOTICE OF TRANSMITTAL TO DDC
This technical report has been reviewed and is approved for public release IAW AFR 190-12 (7b).
Distribution is unlimited.
A. D. BLOSE
Technical Information Officer

ABSTRACT

The objectives of this research were to more clearly understand the roles of microstructure and plastic deformation in fatigue crack initiation and propagation in selected aluminum-base alloys with the anticipation that such information will point the way toward aluminum alloys with improved fatigue resistance. Specifically studied were:

1) "Fatigue Crack Initiation and Microcrack Growth in 2024-T4 and 2124-T4 Aluminum Alloys"

A metallograph was mounted directly on a closed-loop electro-hydraulic testing unit and initiation of fatigue cracks was directly observed on polished notches at magnifications up to 800X in aluminum alloys 2024 and 2124 in the T4 condition. The latter is a high purity coarser grain-sized version of 2024 and contains many fewer constituent particles. At high stresses on the notch surface, the fatigue cracks initiated on coarse slip lines in both. At low stresses almost all of the cracks in 2024 initiated in the matrix adjacent to constituent particles. In 2124 at low stresses 50% of the cracks initiated near constituent particles and 50% in the matrix not near constituent particles. The probability that a constituent particle in 2024 initiates a fatigue crack falls off very rapidly as the particle size decreases below 7 μm. Growth of microcracks is impeded by grain boundaries. The fatigue resistance of 2024 is better at high stresses because of the finer grain size; 2124 is better at low stresses because of the reduced constituent particle content.

2) "Role of Plastic Work in Fatigue Crack Propagation in Metals"

The plastic work required for a unit area of fatigue crack propagation U was measured by cementing tiny foil strain gages ahead of propagating fatigue cracks and recording the stress-strain curves as the crack approached. Values of U and plastic zone size in aluminum alloys, 7050-T76, 7050-T4, 2024-T4, 2219-T861, 2219 overaged, and Al-6.3 wt.% Cu-T4, and a binary Ni-base alloy with 7.2 wt.% Al are herein reported. The results are discussed along with U values for three steels measured in this laboratory in a program supported by the American Iron and Steel Institute. When U is compared to the fatigue crack propagation rate at constant ΔK along with strength and modulus, the conclusion is drawn that U is one of the parameters which determines the rate of fatigue crack propagation. A beginning was made on relating U to microstructure. "Homogeneous" plastic deformation in the plastic zone ahead of the crack yields higher values of U. All of the present data fit an empirical equation for the fatigue crack propagation rate

$$\frac{dc}{dN} = \frac{(2.7 \pm 1.2)\ 10^{-3}\ \Delta K^4}{\mu\ \sigma_y^2 U} \quad \text{m/cycle}$$

where μ is the shear modulus and σ_y is the 0.2% offset cyclic yield stress.

3) "Fatigue Crack Propagation Rate of 99.99+% Al and 1100 Al Alloy at 298 and 77°K"

The fatigue crack propagation rate of 99.99+% Al and 1100 Al alloy is substantially lower at 77 than at 298°K. This holds for the cold worked as well as the annealed conditions. The origin of the

decrease is a large increase in U on cooling which correlates with the dislocation structure resulting from the cyclic straining. Cells result at 298°K, tangles at 77°K. Direct measurements of U at room temperature fell within the range of the empirical equation given on the previous page.

INTRODUCTION

Since fatigue cracks initiate and propagate by plastic deformation processes which in turn intimately depend on the microstructure, the fatigue resistance of an alloy must depend on its microstructure. This dependence is often obscure because of counterbalancing effects; nevertheless, a more clear understanding of the roles of microstructure in fatigue resistance of aluminum alloys, hopefully, will result in improved, more fatigue resistant alloys.

Fatigue cracks begin as tiny microcracks. Inclusions or constituent particles are known to play a determining role in initiation of such fatigue cracks at low stresses. It was, therefore, decided to do a quantitative study on the relation between constituent particle size and probability of initiation of a fatigue crack at an inclusion in 2024 type aluminum alloys. The mechanism by which fatigue crack initiation is catalyzed by constituent particles was also not clear and experiments were undertaken to try to determine the mechanism. Since grain size was also expected to be an important factor in fatigue crack initiation, the study included alloys of different grain size as well as different impurity contents.

Once microcracks have initiated, they grow or coalesce as a result of the applied cyclic loading into a fatigue macrocrack, which is larger than several grain diameters. Since much of the fatigue lifetime is in the microcrack growth stage and this stage has been studied relatively little, the present investigation of 2024 type alloys also included microcrack propagation.

Theoretical studies of the propagation of fatigue macrocracks have

shown that the rate should be inversely proportional to the alloy's strength and to the plastic work per unit area of fatigue crack. Often, when the strength is increased, the cyclic plastic work or cyclic ductility is decreased so the two effects counteract each other. The plastic work to propagate a unit area of fatigue crack which had never been previously measured was measured in this study and a beginning was made in relating it to microstructure and to the details of the plastic work processes of fatigue crack propagation in aluminum alloys.

Finally, we undertook to verify and explain the 100 fold decrease in the fatigue macrocrack propagation rate in unalloyed Al when the temperature is decreased from 298 to 77°K and also to determine the effects of cold work and small amounts of alloying elements. The secret to low fatigue macrocrack propagation rate alloys is learning how to increase strength without sacrificing cyclic ductility or increasing cyclic ductility at the same strength of alloy. This occurs on cooling and thus the origin of the effect may be of considerable practical importance.

These researches will be reported in the following three separate sections.

1. Fatigue Crack Initiation and Microcrack Growth in 2024-T4 and 2124-T4 Aluminum Alloys

The aluminum alloys 2024 and 2124 were selected for study of the relation of microstructure to the sequence of events which lead to the initiation of fatigue cracks and their growth into macrocracks because they allowed an evaluation of the roles of constituent particles and grain size. A metallographic microscope with magnifications up to 800 times was mounted on the fatigue apparatus for direct observation of the specimen's

surface during cyclic loading.

The 2024 and 2124 aluminum alloys were supplied by the Alcoa Research Center. The former contained 1.2 vol.% S-phase (Al_2CuMg) and 1.1 vol.% β-phase (Cu_2FeAl_7). The 2124 is a high purity version of 2024. By lowering the Fe, Si, and Cu contents and using a high solution treatment, the S-phase particles were essentially eliminated (there were some unidentified 0.5 μm particles at grain boundaries). The volume fraction of β-phase was only approximately 0.2 vol.%. The 2124 alloy had a larger grain size than the 2024 alloy, 45 μm compared to 20 μm in the transverse direction which was normal to the loading direction. The heat treatment was solution treating at 495°C, quenching into ice water and aging at room temperature for at least seven days (T4 treatment). This gave a 0.2% offset yield stress of 314 MN/m^2 for 2024(T4) and 298 MN/m^2 for 2124(T4).

Edge notches 1.8 mm deep and 0.6 mm radius of curvature were carefully machined into the specimens which were 100 × 20 × 3 mm and then the notch was polished with 30 μm and 1 μm diamond paste. A Neuber stress concentration factor, K_n, which includes plasticity, of 2.6 was determined by curve fitting the data of the cycles to initiation of a fatigue crack in notched and un-notched specimens. The stress concentration factor assuming only elastic stresses was 4.4.

Two modes of fatigue crack initiation were observed. One mode was associated with coarse slip lines in the matrix and was not associated with constituent particles. Such cracks initiated in grain interiors and not near grain boundaries. The second mode was associated with constituent particles. The cracks again formed in the matrix and seemed to emanate from the particles. For the cracks near constituent particles,

there was no evidence for debonding between the constituent particles and the matrix. Such debonding associated with cracks was only observed after the cracks were already quite long. Cracks in the particles did not play a role in fatigue crack initiation in these alloys.

The slip band mode alone was observed at high maximum stresses in both 2024 and 2124. As the maximum stress was lowered, a transition stress was reached where fatigue crack initiation began to be observed near particles. With $R = \sigma_{max}/\sigma_{min} = -1$, the maximum stress, $K_n\sigma_{max}$, at the transition was 200 MN/m^2 (75 MN/m^2 nominal stress) for 2124 and 365 MN/m^2 (140 MN/m^2 nominal stress) for 2024. At low maximum stresses ($K_n\sigma_{max}$ = 180 MN/m^2, σ_{max} = 50 MN/m^2), 50% of the cracks were of the slip band type in 2124 but only 5% in 2024.

Not all of the constituent particles in 2024 initiated fatigue cracks at low or intermediate stress levels; at most, 2 to 3% of the particles initiated cracks. An analysis was made of the crack initiation probability vs. particle size for both the S (Al_2CuMg) and β (Al_7Cu_2Fe) phase particles. The fatigue crack initiation probabilities vs. constituent particle size normal to the stress direction for mechanically polished specimens of 2024-T4 are plotted in Fig. 1. Since the rolling direction was parallel to the stress direction, the measured dimension is in the short transverse (thickness) direction. The S particles are more or less spherical, the β particles are elongated in the rolling direction; however, their lengths are proportional to their thicknesses. Data for 228 cracks are included in the figure. The number of cracked particles in each 1 μm incremental thickness element was divided by the particle size distribution (which peaks at 3 μm for the β-phase and below 2 μm for the

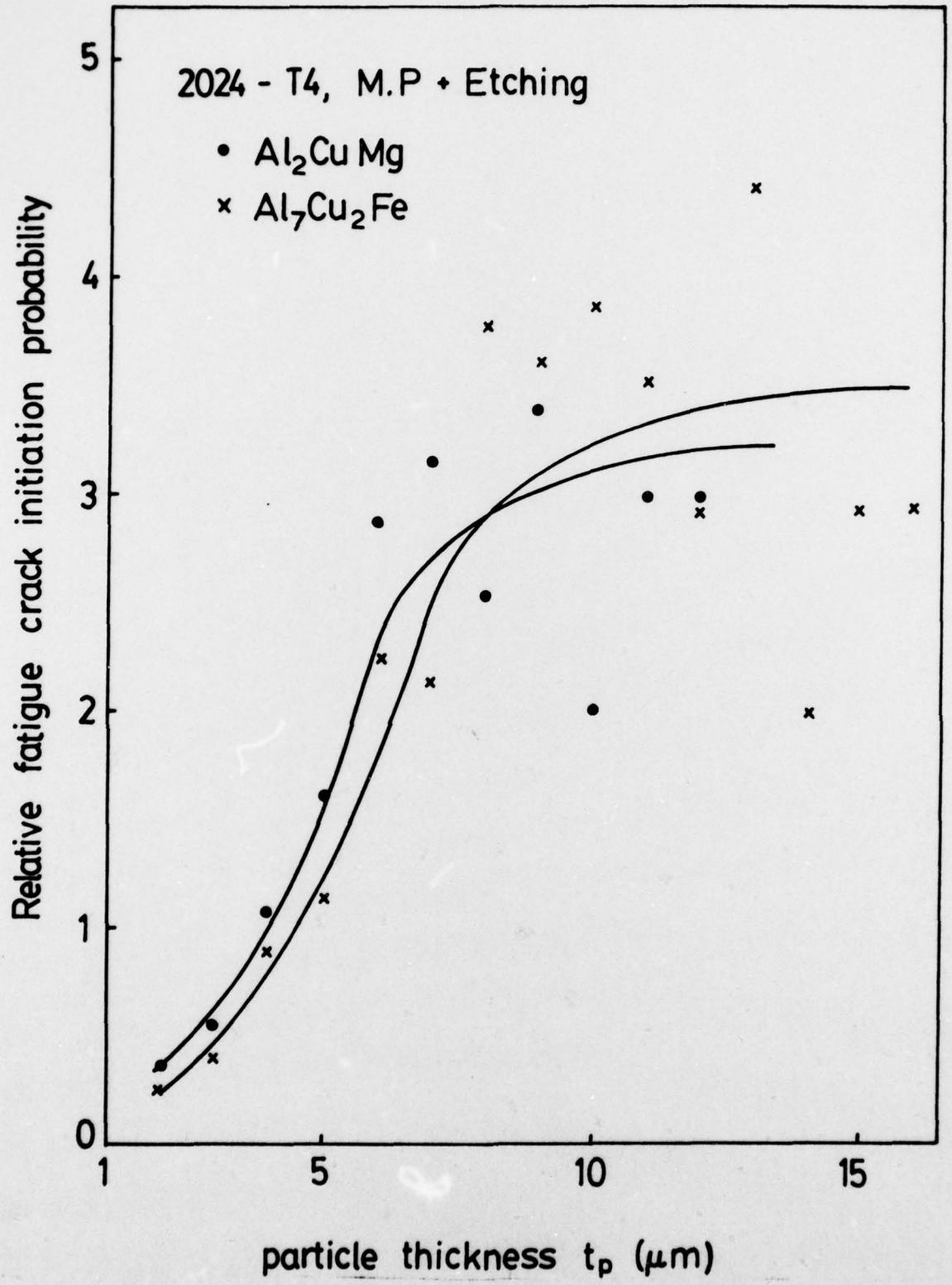

Fig. 1. Relative fatigue crack initiation probability of 2024-T4 mechanically polished vs. constituent particle thickness normal to stress direction. The crack probabilities vs. size were divided by the size distributions to give the data plotted.

S-phase) to give the relative fatigue crack initiation probability. For both types of particles the probability drops very drastically as the thickness decreases below 7 μm and is small for 2 μm. For the larger thicknesses, there is considerable spread in the data due to insufficient number of cracks in this range to give good statistics.

The fatigue crack initiation lifetimes for 2124-T4 and 2024-T4 are compared in Fig. 2. At high stresses, N_{ii} for 2024 is larger than for 2124 due to the smaller grain size of 2024; the resistance to initiation of fatigue cracks on slip lines decreases as the grain size increases. The reverse is true at low stresses due to the smaller constituent particle content of 2124 even though it has a lower yield stress.

It was proposed that intrusions and extrusions which lead to fatigue cracks form more readily where slip bands impinge on particles. Moreover, since many large particles do not initiate cracks, the mechanism must involve a singularity in the matrix as well as the presence of a particle. Slip bands are the most obvious singularities. The decrease in probability that a constituent particle will initiate a fatigue crack as the size decreases below 7 μm may be due to the fact that the probability for a coarse slip band impinging on a particle falls off with the particle size.

Even though the 2124 alloy has many fewer constituent particles than the 2024 alloy studied, there was only a small increase in fatigue crack initiation resistance at low stresses no doubt due to the larger grain size and lower yield stress in the higher purity alloy. Both modes of fatigue crack initiation may be made easier by increase in grain size.

The main crack was usually formed by coalescence of 5 to 10 microcracks. The growth rates of most cracks actually initially decreased

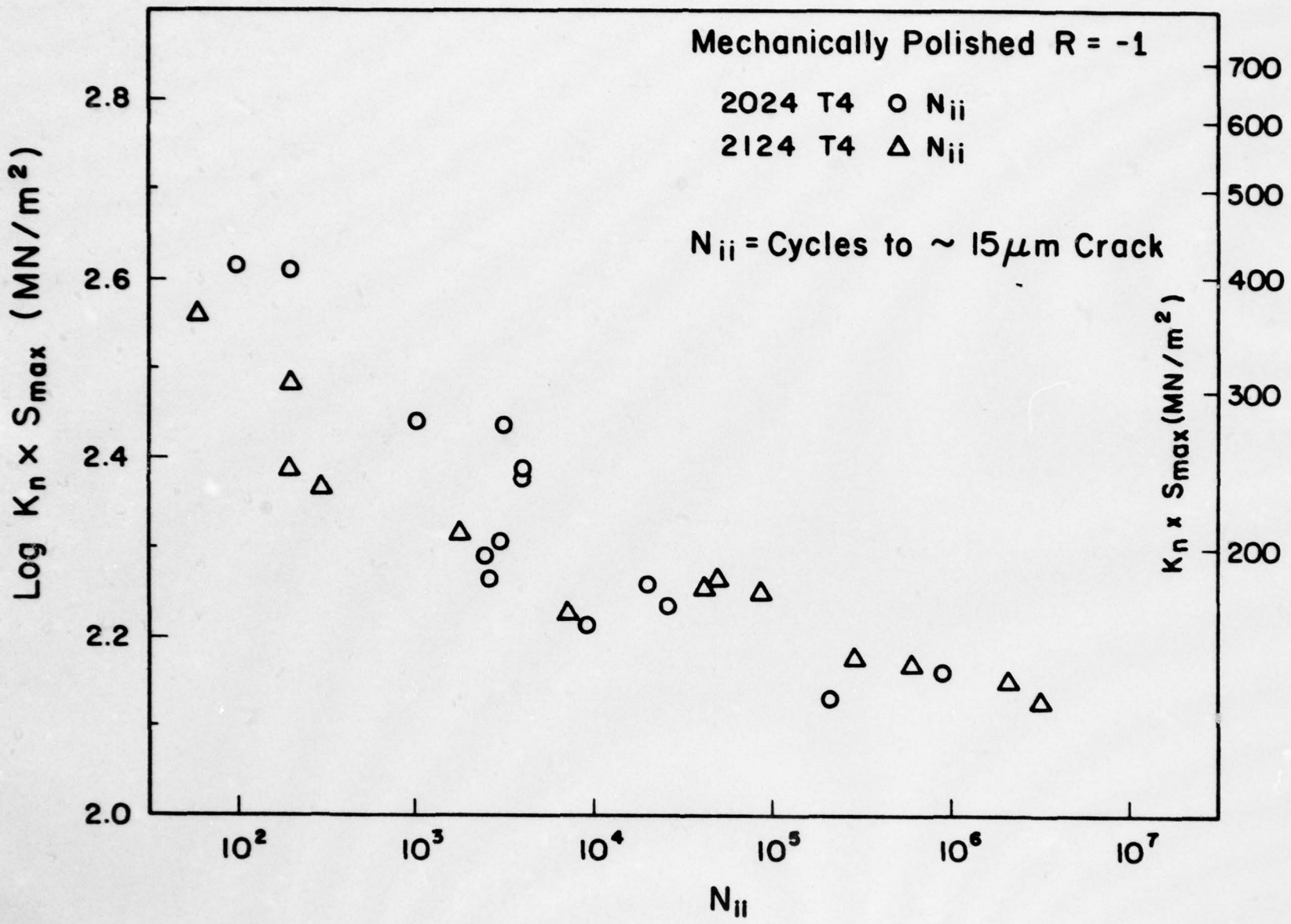

Fig. 2. Cycles to fatigue crack initiation for mechanically polished specimens of 2024-T4 and 2124-T4 vs. $K_n S_{max}$, where S_{max} is the maximum nominal stress.

with N except when coalescence occurred. In a few specimens of 2024 and 2124 at low stress amplitude the major crack formed from a single source without coalescing with other cracks. In these cases, the growth rates generally slowly increased as the cracks spread.

Microcracks were observed to slow down or stop when they neared grain boundaries. In order to quantify the effect, the distances between crack ends and the nearest grain boundaries were measured in 16 specimens of 2024 after many cracks had initiated. The results are shown in Fig. 3. Clearly, most cracks terminated within one to two μm of a grain boundary. This must be because the slip processes which produce crack growth are discontinuous across grain boundaries.

Thus for improved alloys more resistant to fatigue initiation and microcrack propagation, fine grain size and small constituent particle size are desirable.

2. Role of Plastic Work in Fatigue Crack Propagation in Metals

Recently, a technique was developed in this laboratory for measuring the integrated plastic work expended in the plastic zone around a fatigue crack for a unit area of crack advance, U, by cementing tiny foil strain gages ahead of fatigue cracks in center notched panel specimens. The initial results for a high strength low alloy Nb steel and 7050 Al alloy showed that the rate of fatigue crack propagation at constant ΔK, $|dc/dN|_{\Delta K}$, depended approximately on 1/U, as predicted theoretically by a number of researchers. These results have been published (Ikeda, Izumi and Fine). This report will review all of the results to date.

Under this Air Force Grant U has been measured on 7050, 2024 and

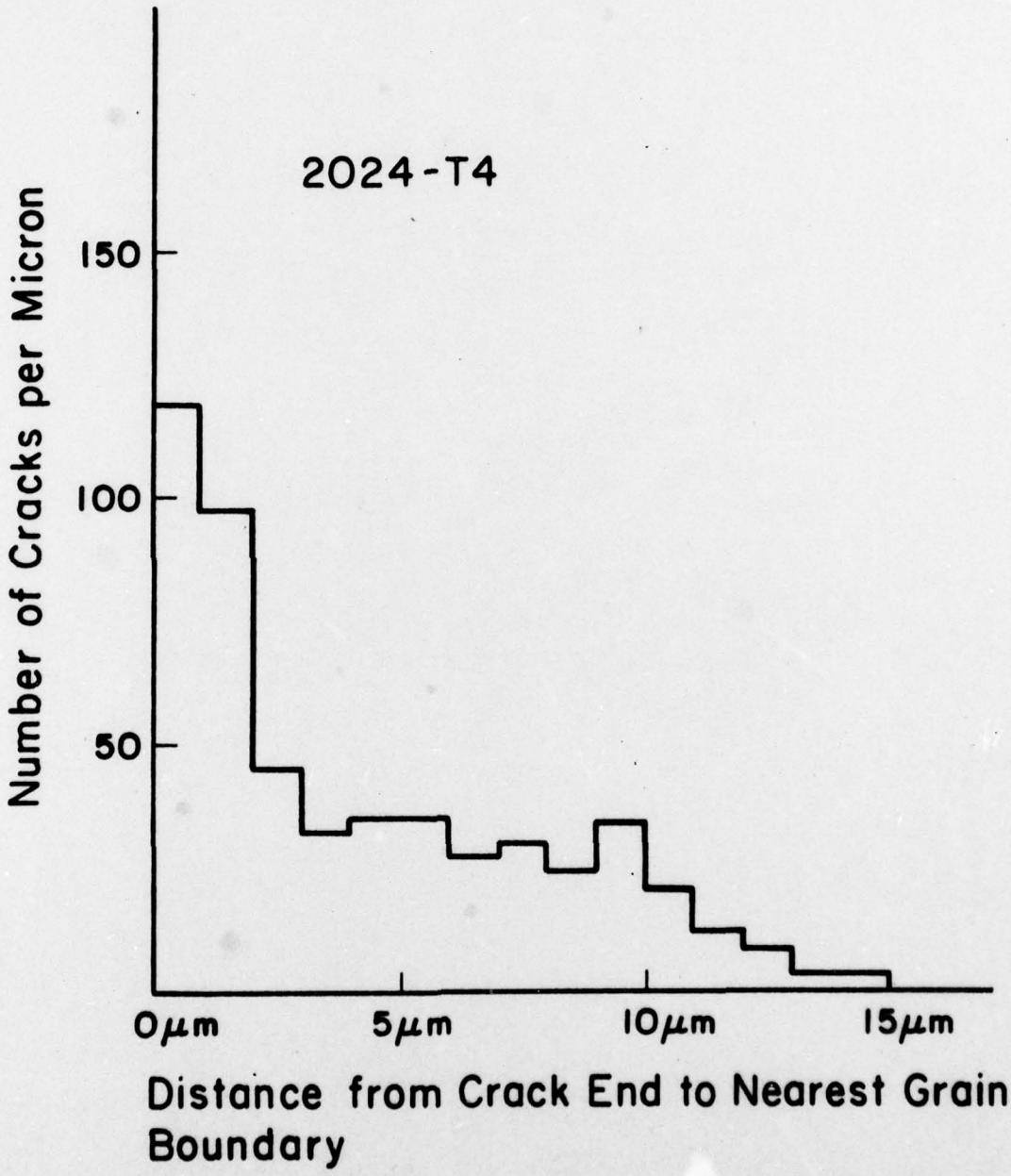

Fig. 3. Distribution of distances between microcrack tips and nearest grain boundaries for lateral spreading of fatigue cracks in polished notches of 1.8 mm deep and 0.6 mm radius of curvature. The data represents 16 specimens of 2024-T4, 536 microcrack tips, $\Delta\sigma$ of 90 to 130 MN/m^2 and 25 to 250 μm crack lengths. The average grain size in the crack spreading direction was 25 μm. The number of cracks are per micron interval between crack ends and nearest grain boundary.

2219 (commercial aluminum alloys) supplied by Alcoa Research Laboratory, a binary Al-6.3 w/o Cu alloy supplied by Kaiser Aluminum and Chemical Corporation Research Laboratory and a binary Ni-7.2 w/o Al alloy supplied by the INCO Research Laboratory. In addition, unalloyed Al and 1100 Al have been measured by P. Liaw, Ph.D. thesis in progress, as described in Section 3 of this report. The technique is fully described in the publications which have resulted from this work. The sources of error and approximations made are fully discussed (Izumi and Fine).

The results are summarized in Table I which also gives the monotonic and cyclic 0.2% offset yield stress, the exponent m in the Paris relation, and A, the constant in the theoretical-empirical relation $da/dN = A(\Delta K)^4/(\mu\, \sigma_y U)$ where μ is the shear modulus. The values for steels in Table I were taken from research in this laboratory supported by the American Iron and Steel Institute.

The fatigue crack propagation rates, $|dc/dN|_{\Delta K}$, for the 2024-T4 and 6.3 w/o Cu-Al alloys in Table I are considerably faster than the rates for the Nb-doped HSLA steel. These differences in $|dc/dN|_{\Delta K}$ cannot be explained by a difference in the shear modulus or σ_y' but can be explained by the differences in the plastic work U.

The value of U for the 2024 alloy is the highest of those for the commercial Al alloys studied while its $|dc/dN|_{\Delta K}$ is the lowest. The large differences in $|dc/dN|_{15.5}$ between the 7050-T76 Al alloy on the one hand and the Ni-base alloy and HSLA steel on the other correlate with the large differences in U. In view of these results, U is obviously playing a determinative role for the rate of fatigue crack propagation.

TABLE I.

U VALUES AND MECHANICAL PROPERTIES

	ΔK $MN/m^{\frac{3}{2}}$	dc/dN m/cycle	U J/m^3	σ_y' MN/m^2	σ_y MN/m^2	m	A
7050 Al T76*	15.5	30×10^{-8}	0.63×10^5	510	470	4.0	2.3×10^{-3}
7050 Al T4*	12.4	30	0.54	410	320	3.5	2.8
Al-6.3 w/o Cu T4	12.4	4.7	5.8				1.6
	10.8	2.0	6.1	230	130	4.0	1.2
	9.3	1.2	10.5				2.3
2024 Al T4	15.5	14	3.2	390	300	3.0	3.1
	7.8	1.6	2.6				4.4
2219 Al T861	15.5	25	1.6	370	350	4.0	2.5
	7.8	1.5	2.4				3.5
2219 Al overaged	15.5	32	1.4	260	270	4.0	1.4
	9.3	6.8	2.1				3.4
Ni-7.2 w/o Al Aged 2 days, 625°C	15.5	2.0	4.8	670	440	4.5	6.3
Nb-doped HSLA steel*	19.5	3.7×10^{-8}	12				2.7
	15.5	1.7	8	340	360	3.5	2.1
	12.4	0.8	12				3.5
	9.3	0.3	6				2.1
Steel - Aged 13 min, 500°C**	19.5	1.8	3.4	710	880	3.5	1.6
Steel - Aged 200 min, 500°C**	19.5	5.6	1.3	780	950	3.0	2.3

* Ikeda, Izumi and Fine[1]
** Ikeda, Sakai and Fine[16]

dc/dN = fatigue crack propagation rate
U = total hysteretic plastic work per unit area
σ_y' = 0.2% offset cyclic yield stress
σ_y = 0.2% offset monotonic yield stress
m = Paris exponent, i.e., $dc/dN = C(\Delta K)^m$
A = constant in Eq.(1)

Specimen thicknesses were 2.3 to 3 mm
Dry argon atmosphere

The Al-6.3 w/o Cu alloy aged at room temperature contains both GPI (Guinier-Preston zones) and θ phase particles. The excess copper over the solubility limit forms θ particles which are 5 to 10 μm in diameter with a mean spacing of about 50 μm. The presence of GP zones tends to give inhomogeneous deformation with coarse planar slip bands. The presence of the large θ particles, however, make the plastic deformation more uniform throughout the specimen, since the θ particles are not penetrable by dislocations and thus dislocations must bend or cross slip around them giving a higher work hardening rate. We propose that this deformation mechanism is the origin of the relatively high U for this alloy. The value of U for 7050 Al alloy is relatively small possibly because few dispersed particles are present. Unlike the 7050 alloy, the 2024 Al alloy has S-phase and Al_7Cu_2Fe constituent particles. The larger value of U for 2024 may in part result from the constituent particles. The GPI zones for the 7050-T4 alloy are spherical while those in 2024-T4 Al are platelets. The higher U in the 2024-T4 alloy may possibly partly result from a greater difficulty for dislocations to avoid cutting platelets than spheres.

The large increase (50%) of σ_y' and σ_y in the Ni-Al alloy is noteworthy (Table I). The aging treatment used gives aligned cube-shaped γ′ precipitates roughly 100Å on a side. The flow stress increase due to cycling may be due to the disordering and creation of antiphase boundaries in the γ′ particles.

Theoretical equations for the fatigue crack propagation rate may be classified into mainly two types: (a) $|dc/dN|_{\Delta K} \sim (\Delta K)^4$ and (b) $|dc/dN|_{\Delta K} \sim (\Delta K)^2$. Experimentally, the exponent on ΔK, m, ranges from

2 to 8. For data for fatigue crack propagation compiled by Frost, Marsh and Pook (Metal Fatigue, Clarendon Press, Oxford, 1974), the average value for 14 alloys is 3.94 with a standard deviation of ± 0.86. For the 8 alloys and treatments given in Table I, the m values ranged from 3 to 4.5 giving m = 3.7 ± 0.5. Thus (a) seems to be the best fit for the present set of data. Theoretically, $dc/dN = \frac{A\ \Delta K^4}{\mu U \sigma'}$ is expected.

Table I also gives the proportionality constant A for the 8 alloys and ΔK's studied assuming that σ', the 0.2% offset cyclic yield stress, is the appropriate strength parameter. The average value of A is 2.7×10^{-3} with a standard deviation of $\pm 1.2 \times 10^{-3}$ giving

$$\frac{da}{dN} = \frac{(2.7 \pm 1.2)\ 10^{-3}\ \Delta K^4}{\mu\ \sigma_y'\ U} \quad .$$

More measurements are needed, of course, to establish the ranges of validity of the equation.

The plastic work U is thought to be an important parameter even for metals which follow $da/dN \sim \Delta K^2$ but, of course, a different theoretical equation would hold for such alloys.

The experimental determination of U using foil strain gages also gives a contour map of the plastic zone. Figure 4 shows a plot of the hysteretic plastic work density contour lines for one-half of the cyclic plastic zone for overaged 2219 at $\Delta K = 9.3\ MN/m^{\frac{3}{2}}$. The cyclic plastic zone extends further from the crack tip at 45° than at 0 or 90°. Along the crack direction the cyclic plastic zone size is approximately 500 μm. The 0.2% offset cyclic yield stress is usually introduced into theoretical and empirical equations for the size of the plastic zone

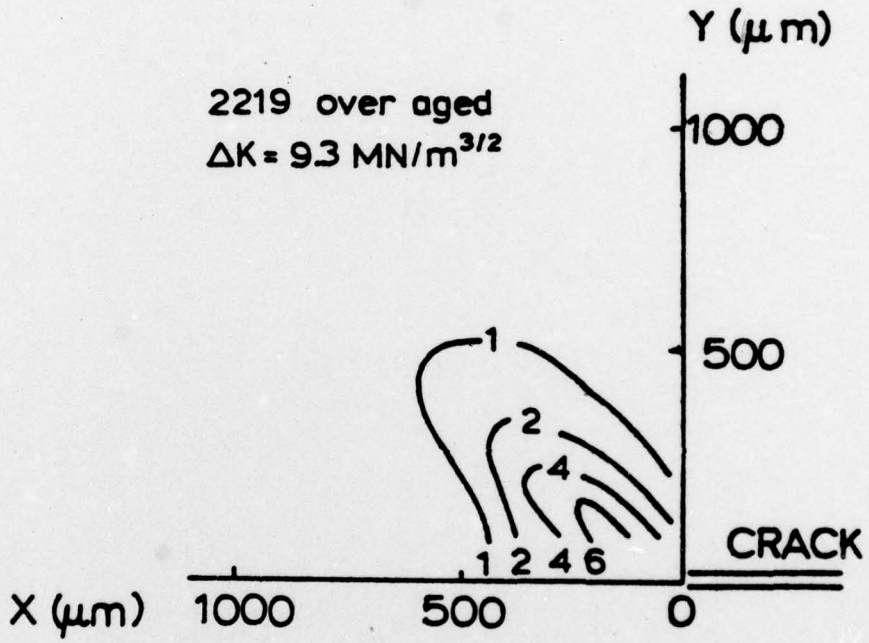

Fig. 4. Equi-hysteretic plastic work density lines for 2219-overaged Aℓ alloy. In sequence toward the origin, the numbers are 1,2,4, and 6 × 10^{11} J/m^4.

(e.g., Rice's formula, $r_p = (\pi/64)(\Delta K/\sigma_y')$). In the present case the appropriate yield stress is the minimum stress to give to and fro dislocation motion, σ_h, and it defines the boundary of the hysteretic plastic zone about a fatigue crack. This is obviously larger (~ 4 times) than the plastic zone computed using the 0.2% offset cyclic yield stress. Values of the present plastic zone sizes $2r^h_{max}$ are given in Table II. There is good correlation between the size of this cyclic plastic zone and U (or $|da/dN|_{\Delta K}$). Note that the nickel-base alloy has a surprisingly large plastic zone size even though σ_h is rather large.

3. Fatigue Crack Propagation Rate of 99.99+% Al and 1100 Al Alloy at 298 and 77°K

An investigation of the fatigue crack propagation rate of 99.99+% Al and 1100 Al alloy at 298 and 77°K was undertaken to learn more about the very large decrease in fatigue crack propagation rate which occurs on cooling Al from room temperature to liquid nitrogen temperature. The impetus for this investigation was partly the expectation that the information developed would be helpful for developing Al alloys with lower propagation rates at room temperature.

The fatigue crack propagation rates for each alloy and each condition studied at 77°K and at 298°K are given in Fig. 5. The very large decrease in rate from cooling is not an effect of environment since the room temperature measurements were done in dried argon while the specimens were immersed in liquid nitrogen for the 77°K tests. The Paris exponents ranged from 3.9 to 4.7.

In joint research with M. Kiritani and S. Ono of Osaka University, Japan, the large reduction in fatigue crack propagation rate was related

TABLE II.

PLASTIC ZONE SIZES

	ΔK $MN/m^{\frac{3}{2}}$	$2r^h_{max}$ μm	σ^h MN/m^2
7050-T76	15.5	630	130
7050-T4	12.4	530	150
Al-6.3% Cu	9.3	780	100
	12.4	1050	100
2024-T4	7.8	680	150
	15.5	910	150
2219-T861	7.8	630	110
	15.5	1080	110
2219-OA	9.3	860	110
	15.5	1100	110
Ni-7.2% Al	15.5	1280	190

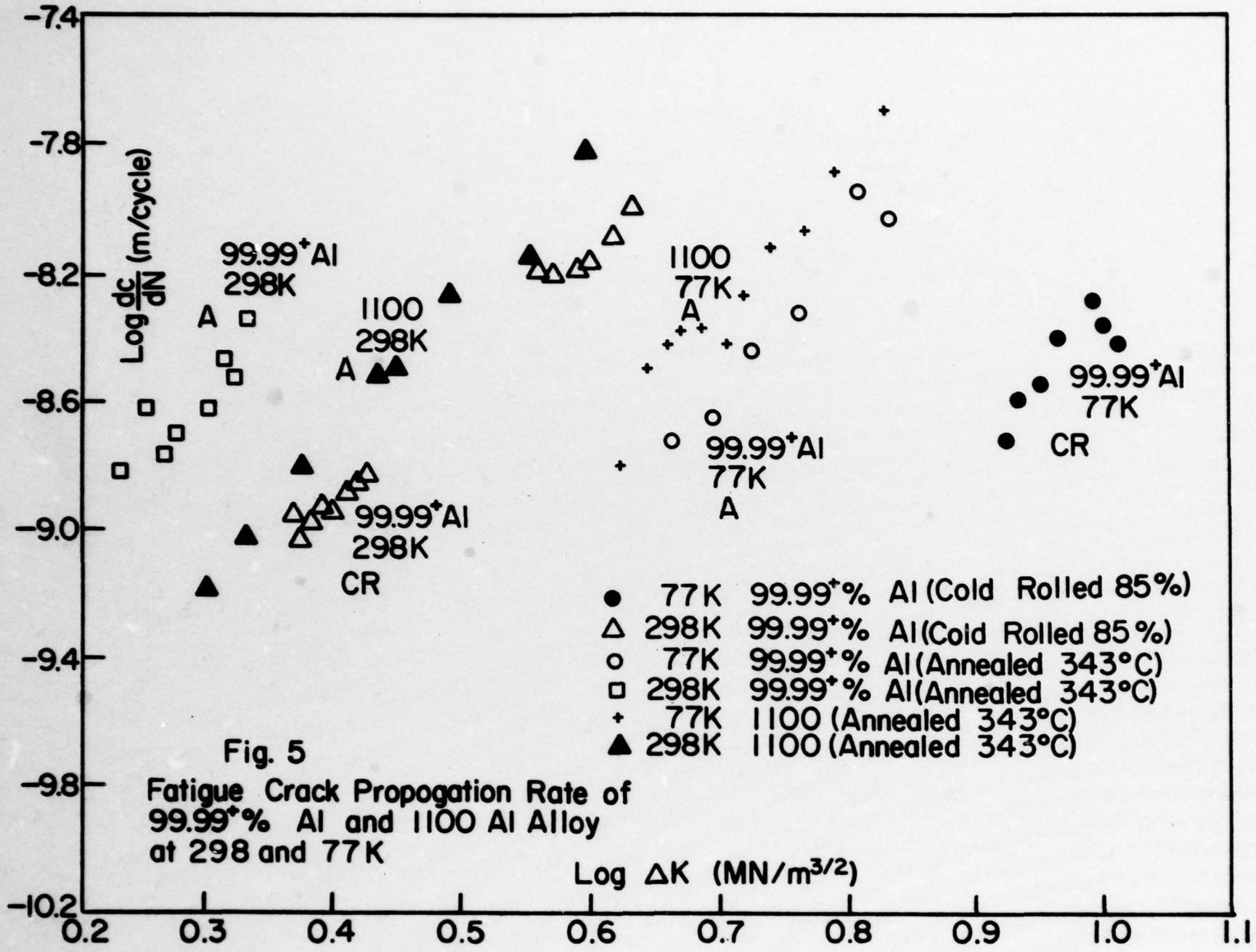

Fig. 5

Fatigue Crack Propogation Rate of 99.99+% Al and 1100 Al Alloy at 298 and 77K

to the difference in dislocation structure which results from cyclic straining at 298°K and 77°K. Cells form in the former, tangles in the latter. The higher dislocation density and more homogeneous distribution of dislocations at 77°K are expected to give a larger value of plastic work to propagate a unit area of fatigue crack U. Using the empirical equation in Section 2 of this report, very large differences in U at the two temperatures are predicted, as shown in Table III.

Using the strain gage technique, U was measured in cold rolled 99.99+ Al and annealed 1100 at room temperature. These values are also given in Table III and the agreement is within a factor of three of the calculated values. The A values for both are 3.4×10^{-3} which is well within the standard deviation range of the empirical equation of Section 2 showing that this empirical equation holds for pure Al and 1100 alloy as well.

It is noted that U values for 99.99+% Al and 1100 Al even at 298°K are considerably larger than for the precipitation hardened Al alloys. Thus alloying elements and impurities reduce U but the σ_y' term in the empirical equation dominates so that the precipitation hardened alloys have much slower rates at 298°K than unalloyed aluminum. If the strengthening can be achieved with less reduction in U, then alloys more resistant to fatigue crack propagation would result.

Fig. 1. Relative fatigue crack initiation probability of 2024-T4 mechanically polished vs. constituent particle thickness normal to stress direction. The crack probabilities vs. size were divided by the size distributions to give the data plotted.

TABLE III.

Comparison of $\left|dc/dN\right|_{\Delta K = 2\ MN/m^{\frac{3}{2}}}$ and Calculated U

		σ_y (0.2%	$\left\|\frac{dc}{dN}\right\|_{\Delta K = 2\ MN/m^{\frac{3}{2}}}$	U^{**}_{calc}	U_{meas}
99.99*					
298°K	annealed	15 MN/m^2	2.7×10^{-9} m/cycle	2.6×10^{6} J/m^2	
77°K	annealed	20	2.6×10^{-11}*	1.5×10^{8} J/m^2	
298°K	cold-rolled	77	4.2×10^{-10}*	6.0×10^{5} J/m^2	1.8×10^{6} J/m^2
77°K	cold-rolled	97	3.7×10^{-12}*	4.2×10^{7} J/m^2	
1100					
298°K		31	6.8×10^{-10}	2.2×10^{6} J/m^2	1.2×10^{6} J/m^2
77°K		49	1.1×10^{-11}*	6.2×10^{7} J/m^2	

* extrapolated from higher values of ΔK

** computed from empirical equation, Section II, using 0.2% monotonic yield stress

LIST OF PUBLICATIONS

A. Papers Published Since 1975

1. "Effect of Dispersed Phases on Cyclic Softening of Al-Cu Alloys", J. S. Santner and M. E. Fine, Scripta Met. 9, 1239 (1975).

2. "Fatigue Crack Propagation in Aluminum-Base Copper Alloys", J. S. Santner and M. E. Fine, Met. Trans. A, 7A, 583 (1976).

3. "Origin of Brittle Intergranular Fatigue Fracture in Warm Aged Al-3.6 w/o Cu", J. S. Santner and M. E. Fine, Met. Trans. A, 7A, 601 (1976).

4. "Role of Ductility and Yield Stress in Fatigue Crack Propagation in Metals", M. E. Fine and Y. Izumi, Fourth International Conference on the Strength of Metals and Alloys, Nancy, France, 30 August-3 September 1976, Proceedings Volume 2, p. 468.

5. "Plastic Work During Fatigue Crack Propagation in a High Strength Low Alloy Steel and in 7050 Aluminum Alloy", S. Ikeda, Y. Izumi and M. E. Fine, Eng. Fract. Mech. 9, 123 (1977).

6. "The Hysteretic Plastic Work as a Failure Criterion in a Coffin-Manson Type Relation", J. S. Santner and M. E. Fine, Scripta Met. 11, 159 (1977).

7. "The Strength and Toughness of a Ceramic Reinforced with Metal Wires", J. G. Zwissler, M. E. Fine and G. W. Groves, J. Amer. Cer. Soc. 60, 390 (1977).

8. "The Effect of Temperature on the Fatigue Crack Propagation Rate in Aluminum", P. K. Liaw, M. E. Fine, M. Kiritani and S. Ono, Scripta Met. 11, 1151 (1977).

B. Papers Not Yet Published

1. "Role of Plastic Work in Fatigue Crack Propagation in Metals", Y. Izumi and M. E. Fine. Accepted for publication by Engineering Fracture Mechanics. To appear in November 1978 issue.

2. "Fatigue Crack Initiation and Near-Threshold Crack Growth", M. E. Fine and R. O. Ritchie, Proceedings of the 1978 ASM Materials Science Seminar, Fatigue and Microstructure, 14-15 October 1978, St. Louis, Missouri. To be published.

3. "Energy Considerations in the Fatigue Crack Propagation", Y. Izumi, M. E. Fine and T. Mura. Submitted to Metallurgical Transactions.

B. Papers Not Yet Published (Continued)

4. "Fatigue Crack Initiation and Microcrack Growth in 2024-T4 and 2124-T4 Aluminum Alloys", C. Y. Kung and M. E. Fine. Accepted for publication by Metallurgical Transactions.

5. "Fatigue Properties of 99.99+ and 1100 Al at 298°K and 77°K", P. K. Liaw and M. E. Fine. In preparation.

LIST OF PROFESSIONAL PERSONNEL WHO PARTICIPATED IN THE RESEARCH

Principal Investigator

Morris E. Fine, Walter P. Murphy Professor of Materials Science and Engineering

Post-Doctoral Research Associate

S. I. Kwun, 6/15/78 - 9/30/79

Graduate Students

J. G. Zwissler - Completed Ph.D. June 1976

C. Y. Kung - Completed Ph.D. June 1978

Y. Izumi - Completed Ph.D. June 1978

K. P. Liaw

S. Hirose

J. McKittrick

Secretary

J. Bell (½ time)

DISSERTATIONS

1. "The Effect of Varying the Fiber Parameters on the Fracture Properties of a Ceramic Matrix-Metal Fiber Composite System", J. G. Zwissler, Ph.D. awarded June 1976.

2. "Role of Plastic Work in Fatigue Crack Propagation in Metals", Y. Izumi, Ph.D. awarded June 1978.

3. "Fatigue Crack Initiation and Growth of Microcracks in Commercial Precipitation Hardened Al-Cu-Mg Alloys of Ordinary and High Purity", C. Y. Kung, Ph.D. awarded June 1978.

SECURITY CLASSIFICATION OF THIS PAGE (When Data

REPORT DOCUMENTATION PAGE

READ INSTRUCTIONS BEFORE COMPLETING FORM

1. REPORT NUMBER: AFOSR-TR-78-1518
2. GOVT ACCESSION NO.
3. RECIPIENT'S CATALOG NUMBER
4. TITLE (and Subtitle): "Relation of Structure to Fatigue Properties in Aluminum-Base Alloys"
5. TYPE OF REPORT & PERIOD COVERED: Scientific----Final Rept. 1 Oct 75 ← 30 Sep 78
6. PERFORMING ORG. REPORT NUMBER
7. AUTHOR(s): Morris E. Fine
8. CONTRACT OR GRANT NUMBER(s): AFOSR-76-2892
9. PERFORMING ORGANIZATION NAME AND ADDRESS: Northwestern University, Department of Materials Science and Engineering, Evanston, Illinois 60201
10. PROGRAM ELEMENT, PROJECT, TASK AREA & WORK UNIT NUMBERS: 61102F, 2306A1
11. CONTROLLING OFFICE NAME AND ADDRESS: AFOSR-NE, Building 410, Bolling AFB, Washington, D. C. 20332
12. REPORT DATE: November 6, 1978
13. NUMBER OF PAGES: 23
14. MONITORING AGENCY NAME & ADDRESS (if different from Controlling Office)
15. SECURITY CLASS. (of this report): Unclassified
15a. DECLASSIFICATION/DOWNGRADING SCHEDULE

16. DISTRIBUTION STATEMENT (of this Report)

Approved for public release; distribution unlimited

17. DISTRIBUTION STATEMENT (of the abstract entered in Block 20, if different from Report)

18. SUPPLEMENTARY NOTES

19. KEY WORDS (Continue on reverse side if necessary and identify by block number)

Fatigue, precipitation hardened aluminum alloys, constituent particles, fatigue crack initiation, fatigue crack propagation

20. ABSTRACT (Continue on reverse side if necessary and identify by block number)

Initiation of fatigue cracks was directly observed at magnifications up to 800 times in aluminum alloys 2024 and 2124. The latter is of higher purity and coarser grained. At low stresses the cracks in 2024 initiated in the matrix near constituent particles. This occurred less in 2124 giving a higher fatigue resistance. The probability that a constituent particle initiates a fatigue crack falls off very rapidly as the particle size decreases below 7 microns. Growth of microcracks is impeded by grain boundaries.

(continued)

DD FORM 1 JAN 73 1473 EDITION OF 1 NOV 65 IS OBSOLETE

260810

UNCLASSIFIED
SECURITY CLASSIFICATION OF THIS PAGE (When Data Entered)

20.

The plastic work required for a unit area of fatigue crack propagation was measured by cementing tiny foil strain gages ahead of propagating fatigue cracks and recording the stress-strain curves. The data for six aluminum alloys, three steels and one nickel alloy fit an empirical equation for the fatigue crack propagation rate showing it is inversely proportional to the plastic work, yield strength squared and the shear modulus.

The fatigue crack propagation rate of aluminum is substantially lower at 77 than at 298 degrees Kelvin. The origin of the decrease is a large increase in plastic work. Dislocation cells result from cyclic straining at 298 degrees Kelvin, tangles at 77 degrees Kelvin.